Physica C 190 (1992) 597–605
North-Holland

PHYSICA C

Crystal structures of stage-n iodine-intercalated compounds $IBi_{2n}Sr_{2n}Ca_nCu_{2n}O_x$

N. Kijima [1] and R. Gronsky

National Center for Electron Microscopy, Materials Sciences Division, Lawrence Berkeley Laboratory, University of California, Berkeley, CA 94720, USA

X.-D. Xiang, W.A. Vareka, A. Zettl, J.L. Corkill and Marvin L. Cohen

Department of Physics, University of California, and Materials Sciences Division, Lawrence Berkeley Laboratory, Berkeley, CA 94720, USA

Received 23 September 1991

The crystal structure of stage-3 iodine-intercalated superconducting $IBi_6Sr_6Ca_3Cu_6O_x$ has been determined by transmission electron microscopy to belong to the space group Pma2 with lattice parameters $a=5.4$ Å, $b=5.4$ Å and $c=49.4$ Å. Iodine atoms intercalated between every three Bi–O bilayers expand the distance between the Bi–O layers by 3.6 Å and alter the atomic stacking across Bi–O layers from the staggered configuration characteristic of host superconducting $Bi_2Sr_2CaCu_2O_x$ to an aligned configuration characteristic of stage-1 iodine-intercalated superconducting $IBi_2Sr_2CaCu_2O_x$. Higher-stage intercalation has also been observed as stacking faults which predominantly contain both stage-2 and stage-3 phases. The space groups and c-axis dimensions of the higher-stage phases have been deduced to be Pma2 with $c=3.6+15.3n$ Å when stage number n is odd, and Bbmb with $c=2(3.6+15.3n)$ Å when n is even.

1. Introduction

Recently, a number of stage-1 iodine-intercalated $Bi_2Sr_2Ca_{n-1}Cu_nO_x$ ($n=1, 2, 3$) superconductors and a stage-2 iodine-intercalated $IBi_4Sr_4Ca_2Cu_4O_x$ were discovered, and the superconducting response of these materials was related to the amount of lattice expansion induced along the c-axis due to intercalation [1–5]. Beginning with host superconductors $Bi_2Sr_2Ca_{n-1}Cu_nO_x$ ($n=1, 2, 3$), iodine was intercalated between every set of Bi–O bilayers at temperatures in the range of 150 to 200°C for times between 10 and 15 days, while iodine was intercalated into every other Bi–O bilayer of a host superconductor $Bi_2Sr_2CaCu_2O_x$ at 300°C for times between 10 and 15 days. It was found from the temperature dependence of the AC and DC magnetic susceptibility that the stage-1 iodine-intercalated compounds behave as bulk superconductors with 2 to 10 K lower superconducting transition temperatures than those of the host materials and that the stage-2 iodine-intercalated superconducting $IBi_4Sr_4Ca_2Cu_4O_x$ has 5 K higher T_c than the stage-1 iodine-intercalated superconducting $IBi_2Sr_2CaCu_2O_x$. The crystal structures of the stage-1 iodine-intercalated $IBi_2Sr_2CaCu_2O_x$ and stage-2 iodine-intercalated $IBi_4Sr_4Ca_2Cu_4O_x$ have been determined by X-ray diffraction analysis [2,3] and transmission electron microscopy [3–5]. These analyses showed that iodine atoms intercalate between the Bi–O bilayers, with a corresponding expansion along the c-axis of 3.6 Å for each Bi–O bilayer, and that the intercalated iodine layers occupy epitaxial sites with respect to the adjacent Bi–O layers, but intercalated iodine atoms alter the atomic stacking across Bi–O layers from the staggered configuration characteristic of superconducting $Bi_2Sr_2CaCu_2O_x$ to a registered configuration in $IBi_2Sr_2CaCu_2O_x$ and $IBi_4Sr_4Ca_2Cu_4O_x$. In the crystal structure of the stage-2 iodine interca-

[1] Now at Mitsubishi Kasei Corporation Research Center, 1000 Kamochida-cho, Midori-ku, Yokohama 227, Japan.

lated superconductor, however, the c-axis dimension is 7.1 Å shorter than four times the c-axis dimension of the stage-1 iodine-intercalated superconductor. It was also found from the atomic spacings apparent in the high-resolution transmission electron microscope images of $IBi_2Sr_2CaCu_2O_x$ and $IBi_4Sr_4Ca_2Cu_4O_x$ that the iodine layers bond to their neighboring Bi–O layers by van der Waals interactions.

Many stacking faults have been observed in those crystals which contain the dominant stage-2 iodine-intercalated compound [5]. In some of these crys-

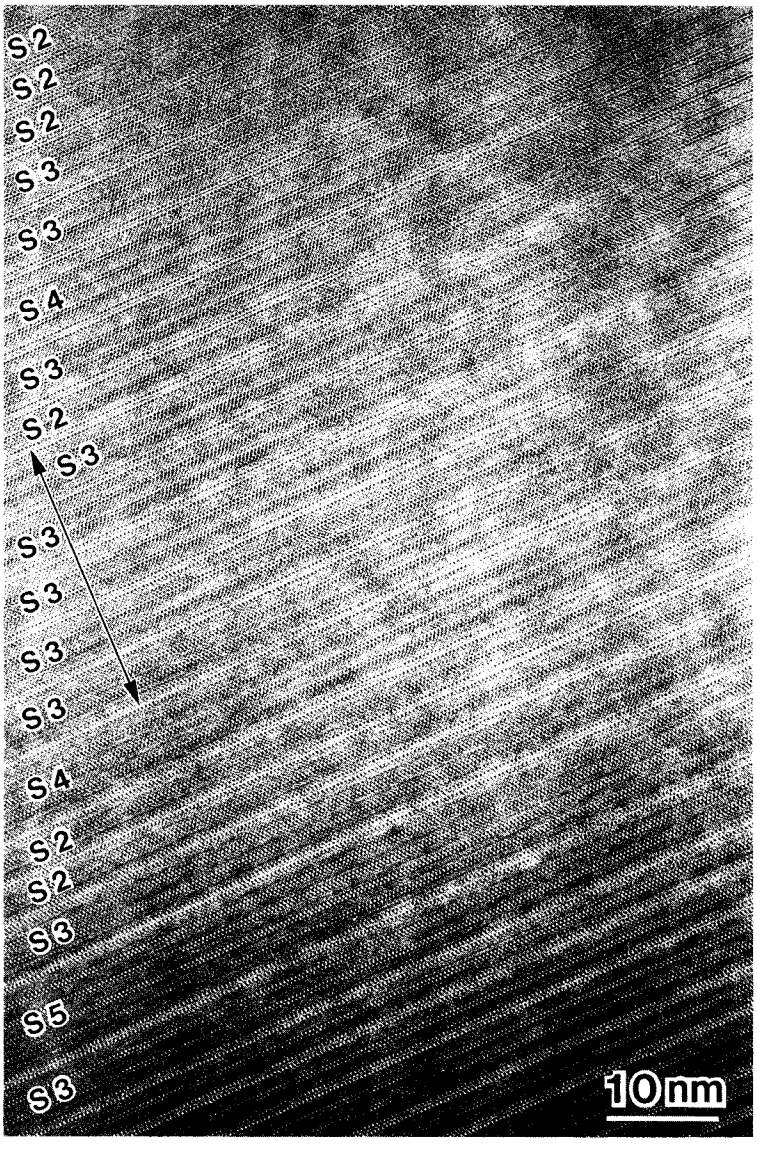

Fig. 1. Phase contrast high-resolution transmission electron microscope image of an area where the stage-3 iodine-intercalated compound is precipitated among the other stage phases. The incident electron beam of the image is along the [$\bar{1}$10] direction. "S2", "S3", "S4" and "S5" represent the iodine-intercalated phases with four different stage numbers which indicate the number of the basic building blocks sandwiched by two iodine layers.

tals, we observed periodically dispersed stage-3 and other higher-stage phases within the stage-2 compound. In order to determine the crystal structures of these higher-stage iodine-intercalated compounds, this study has been undertaken using high resolution transmission electron microscopy.

2. Experimental

Several plate-like crystals of nominal stage-2 iodine-intercalated superconducting $IBi_4Sr_4Ca_2Cu_4O_x$ were prepared by encapsulating iodine and high-quality single crystals of $Bi_2Sr_2CaCu_2O_x$ in a Pyrex® tube under a vacuum of $<10^{-3}$ Torr. Iodine intercalation was carried out at 300°C for 10 days in a uniform-temperature furnace.

Transmission Laue patterns of the iodine-intercalated products were used to orient the crystals for precise cutting into thin wafers, which were subsequently sandwiched between silicon wafers, mechanically thinned and dimpled, and then ion-milled to electron transparency. Ion milling was carried out at 77 K using argon ions accelerated at 3 kV and an incidence angle of 10 degrees. Transmission electron microscopy was performed in the Berkeley JEOL® JEM ARM-1000™ operating at 800 kV. Images were Fourier filtered using the image processing program SEMPER [6], and compared with images simulated by the code NCEMSS [7] at the National Center for Electron Microscopy.

3. Results and discussion

It is commonly observed that stacking faults occur abundantly throughout the stage-2 iodine-intercalated compound. Figure 1 shows a high-resolution transmission electron microscope image of a region wherein stage-3 (S3) stage-4 (S4) and stage-5 (S5) lamellae are dispersed within the stage-2 (S2) matrix. The double arrow identifies a thicker lamella of the stage-3 phase which has the characteristic feature of iodine layers appearing between every third set of Bi–O bilayers. This amount of long range order (≥ 5 unit cells) was never seen for any of the other higher-stage phases.

Figure 2 shows selected area electron diffraction patterns from the same area of the iodine-intercalated crystal, but in two different zone axes. All primary reflections can be indexed on the assumption that this crystal contains both stage-2 (space group Bbmb, lattice parameters $a=5.4$ Å, $b=5.4$ Å and

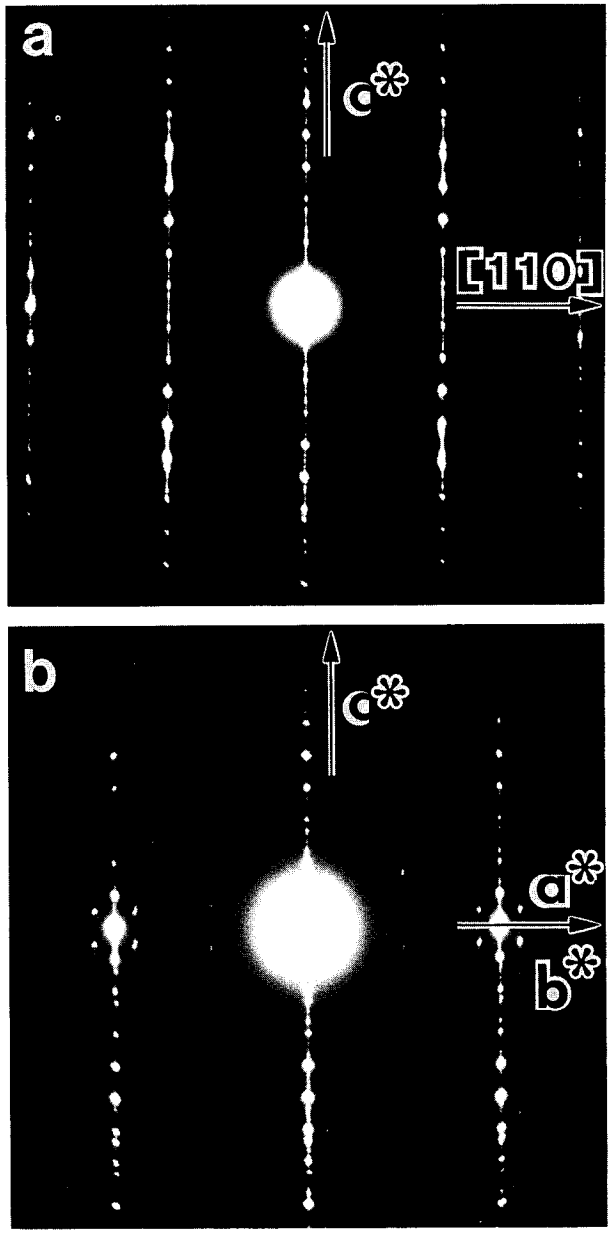

Fig. 2. Selected area electron diffraction patterns of the iodine-intercalated superconductor. (a) [110]–c^* plane, (b) a^*–c^* and b^*–c^* planes.

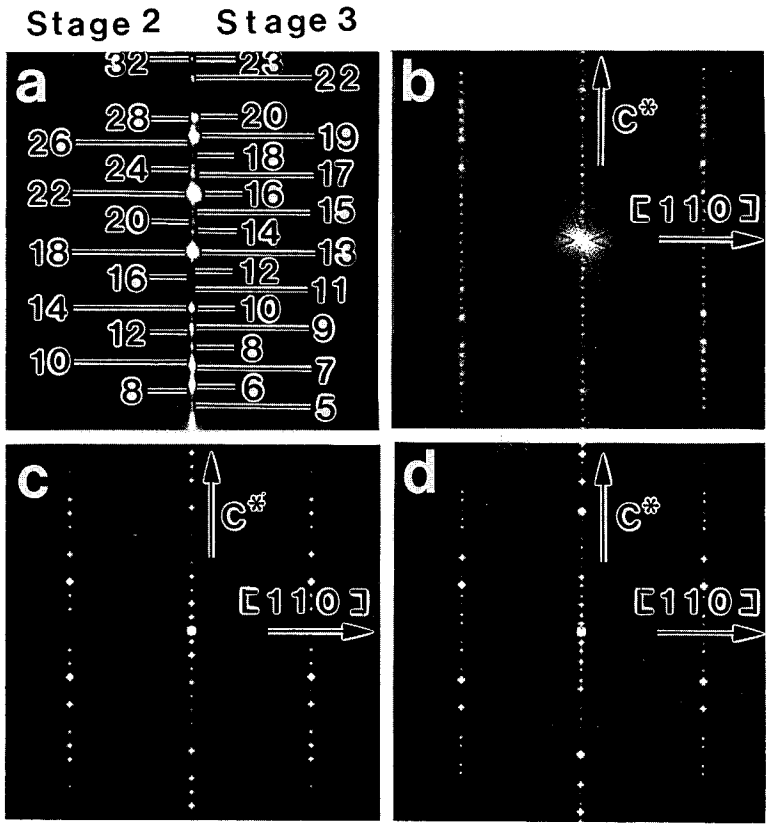

Fig. 3. (a) Magnified version of the selected area electron diffraction pattern shown in fig. 1(a). The l indices of 00l reflections of the stage-2 iodine-intercalated compound are shown on the left of the reflections, while those of the stage-3 iodine-intercalated compound are shown on their right. (b) Electron diffraction pattern Fourier-transformed from the area which includes only the stage-3 iodine-intercalated compound, (c) simulated electron diffraction pattern for the stage-2 iodine-intercalated compound [5], (d) electron diffraction pattern for the stage-3 iodine-intercalated compound simulated with the atomic positions listed in table 1 assuming lattice parameters $a=5.4$ Å, $b=5.4$ Å, $c=49.4$ Å and space group Pma2. Zone axis of all the electron diffraction patterns is $[\bar{1}10]$.

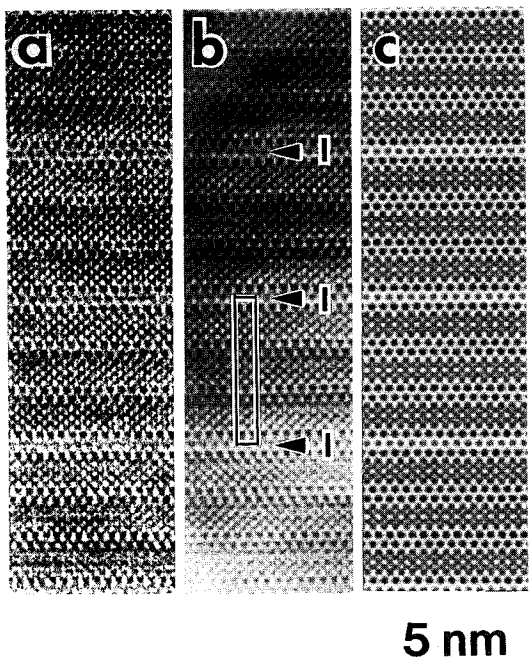

Fig. 4. Phase contrast high-resolution transmission electron microscope image (a), corresponding processed image (b) by means of Fourier filtering, and simulated image (c) using the atomic parameters in table 1. The incident electron beam is along the $[\bar{1}10]$ direction. The specimen thickness is 6 nm. The box shows the unit cell, which includes an iodine layer and three basic building blocks of Bi, Sr, Cu, Ca and oxygen atoms. Compare with fig. 6(d).

Table 1
Atomic positions for the stage-3 iodine-intercalated superconductor $IBi_6Sr_6Ca_3Cu_6O_x$ used in image simulations

Atom	Site	x	y	z
I	2c	0.25	0.75	0.0
Bi(1)	2c	0.25	0.28	0.069
Bi(2)	2c	0.25	0.22	0.313
Bi(3)	2c	0.25	0.78	0.378
Bi(4)	2c	0.25	0.72	0.622
Bi(5)	2c	0.25	0.28	0.687
Bi(6)	2c	0.25	0.22	0.931
Sr(1)	2c	0.25	0.75	0.123
Sr(2)	2c	0.25	0.75	0.258
Sr(3)	2c	0.25	0.25	0.432
Sr(4)	2c	0.25	0.25	0.568
Sr(5)	2c	0.25	0.75	0.742
Sr(6)	2c	0.25	0.75	0.877
Cu(1)	2c	0.25	0.25	0.157
Cu(2)	2c	0.25	0.25	0.224
Cu(3)	2c	0.25	0.75	0.467
Cu(4)	2c	0.25	0.75	0.533
Cu(5)	2c	0.25	0.25	0.776
Cu(6)	2c	0.25	0.25	0.843
Ca(1)	2c	0.25	0.75	0.191
Ca(2)	2c	0.25	0.25	0.500
Ca(3)	2c	0.25	0.75	0.809
O(1)	2c	0.25	0.78	0.069
O(2)	2c	0.25	0.72	0.313
O(3)	2c	0.25	0.28	0.378
O(4)	2c	0.25	0.22	0.622
O(5)	2c	0.25	0.78	0.687
O(6)	2c	0.25	0.72	0.931
O(7)	2c	0.25	0.25	0.110
O(8)	2c	0.25	0.25	0.271
O(9)	2c	0.25	0.75	0.420
O(10)	2c	0.25	0.75	0.581
O(11)	2c	0.25	0.25	0.729
O(12)	2c	0.25	0.25	0.890
O(13)	2a	0.0	0.0	0.157
O(14)	2a	0.0	0.0	0.224
O(15)	2a	0.0	0.0	0.467
O(16)	2a	0.0	0.0	0.533
O(17)	2a	0.0	0.0	0.776
O(18)	2a	0.0	0.0	0.843
O(19)	2b	0.0	0.5	0.157
O(20)	2b	0.0	0.5	0.224
O(21)	2b	0.0	0.5	0.467
O(22)	2b	0.0	0.5	0.533
O(23)	2b	0.0	0.5	0.776
O(24)	2b	0.0	0.5	0.843

$c=68.5$ Å), and stage-3 (space group Pma2, lattice parameters $a=5.4$ Å, $b=5.4$ Å and $c=49.4$ Å) phases. Figure 3(a) shows a magnified segment of

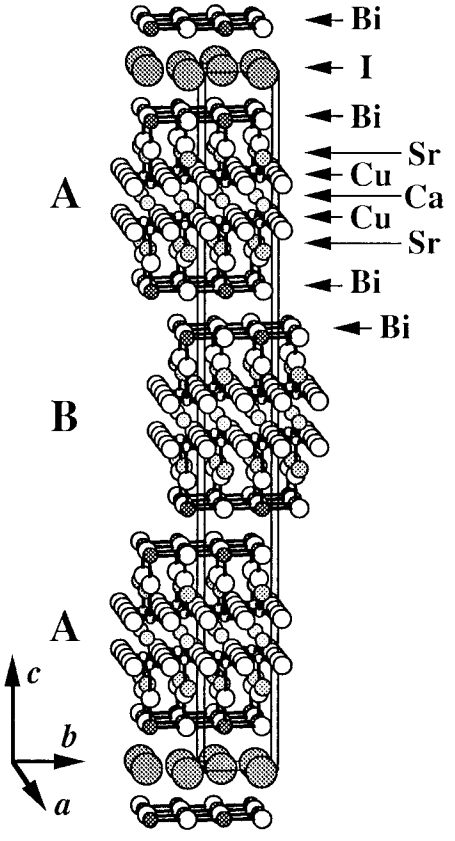

Fig. 5. Crystal structure of the stage-3 iodine-intercalated compound $IBi_6Sr_6Ca_3Cu_6O_x$.

fig. 2(a) featuring the 00*l* reflections, verifying the presence of only these two phases and no higher stage intercalates. Comparison with fig. 3(b), a Fourier transform of the region of fig. 1 containing only stage-3 materials, and the simulations in fig. 3(c) of a stage-2 phase diffraction pattern, and fig. 3(d) of a stage-3 phase diffraction pattern, shows good agreement. X-ray diffraction patterns similarly show no evidence of higher-stage intercalates, indicating that only stage-2 and stage-3 iodine-intercalated crystals are thermodynamically stable in a saturated iodine vapor pressure at 300°C.

The *a* and *b* axial lengths of the pristine host material, which has space group Bbmb and lattice parameters $a=5.4$ Å, $b=5.4$ Å and $c=30.6$ Å, are identical to those of all the stage-1, stage-2 and stage-3 iodine-intercalated compounds; however, the *c*-axis dimensions vary from 18.9 Å to 68.5 Å depending

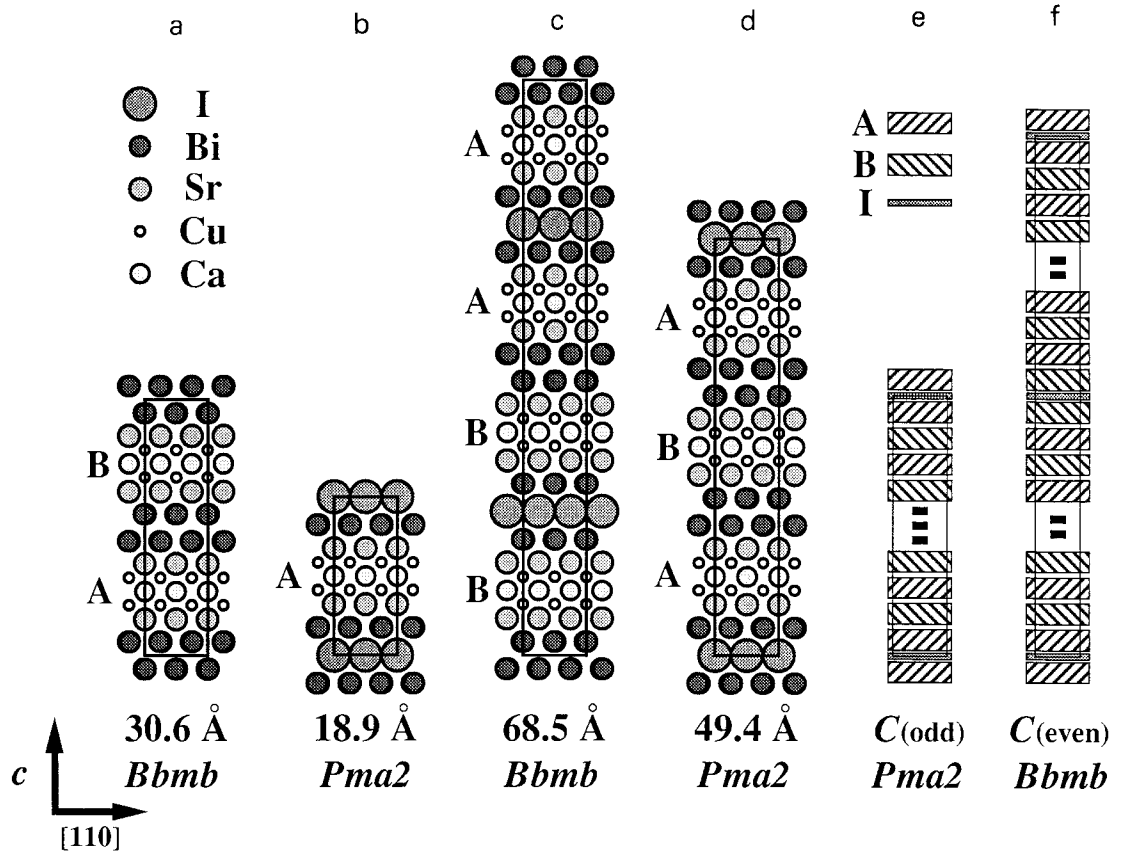

Fig. 6. Comparison of the crystal structures of the host material $Bi_2Sr_2CaCu_2O_x$ (a), stage-1 iodine-intercalated compound $IBi_2Sr_2CaCu_2O_x$ (b), stage-2 iodine-intercalated compound $IBi_4Sr_4Ca_2Cu_4O_x$ (c), stage-3 iodine-intercalated compound $IBi_6Sr_6Ca_3Cu_6O_x$ (d), stage-n iodine-intercalated compounds $IBi_{2n}Sr_{2n}Ca_nCu_{2n}O_x$ when its stage number is odd (e) and even (f). The c lattice parameters C (odd) and C (even) are $m(3.6+15.3n)$ Å, where $m=1$ when n is odd and $m=2$ when n is even.

upon stage number. The c parameter does not linearly increase with stage number, due to the fact that iodine intercalation causes not only the expansion of the distance between the Bi–O layers but also a change in the stacking sequence of the contiguous structure, as revealed in the high resolution images.

Figure 4 shows an original high-resolution transmission electron micrograph (a), corresponding processed image (b) and simulated image (c) of the stage-3 iodine-intercalated compound with a $[\bar{1}10]$ incident beam direction along a 6-nm thick sample. The box in fig. 4(b) shows a unit cell for comparison, and it is observed with excellent agreement among these figures that iodine atoms marked "I" intercalate between every third set of Bi–O bilayers.

Table 1 summarizes the atomic positions used during image simulation; the atomic coordinates of the oxygen atoms in the Bi–O layers were fixed at the center of the adjacent four Bi atoms as they were in previous studies of both the stage-1 and stage-2 iodine-intercalated compounds. Figure 5 schematically depicts the crystal structure of the stage-3 iodine-intercalated superconductor $IBi_6Sr_6Ca_3Cu_6O_x$. As in the host material, the basic building blocks of Bi, Sr, Ca, Cu and oxygen in the stage-3 iodine-intercalated compound are staggered by half of the b axial length across the Bi–O bilayers in the absence of iodine atoms. With iodine intercalation, the basic building blocks are brought into registration across the Bi–O bilayer. Consequently, only the basic build-

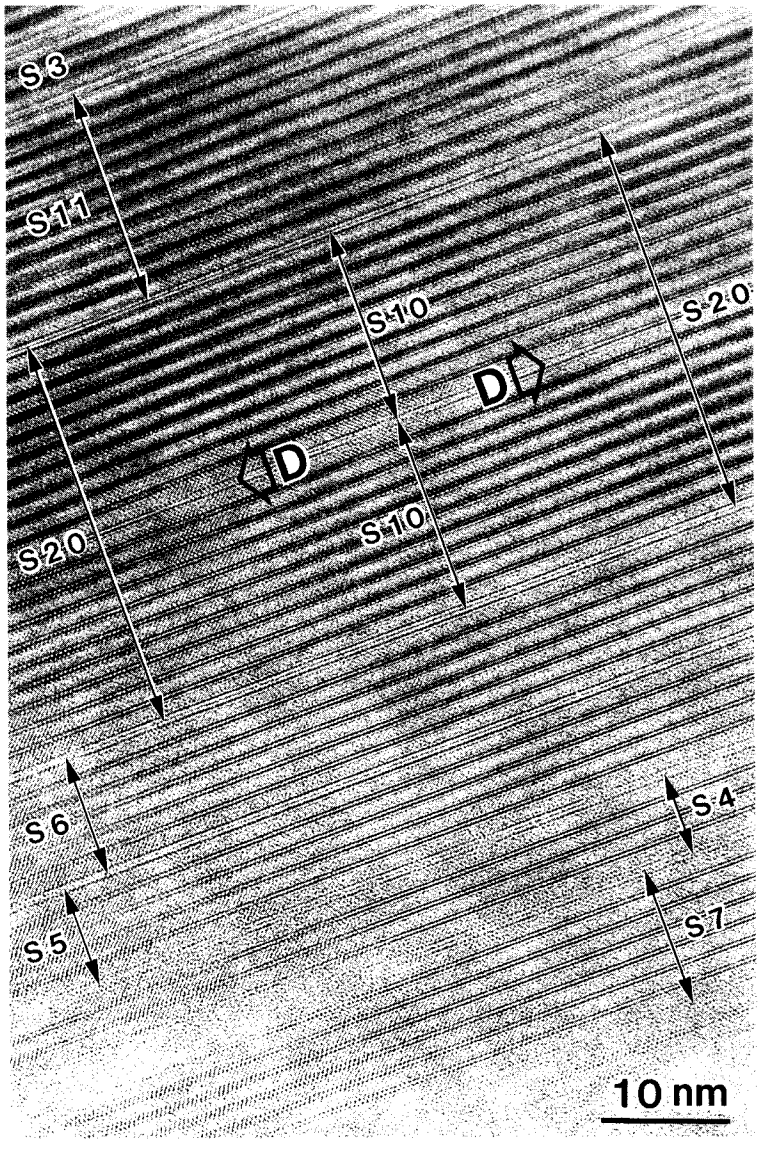

Fig. 7. Phase contrast high-resolution transmission electron microscope image of the area where the higher-stage (> stage-3) iodine-intercalated phases are precipitated in the same crystal that the stage-2 and stage-3 compounds are dominantly precipitated in. The incident electron beam of the images is along the [$\bar{1}$10] direction. "S4", "S5", "S6", "S7", "S10", "S11" and "S20" represent the iodine-intercalated phases with different stage numbers which indicate the number of the basic building blocks sandwiched by two iodine layers.

ing block in the middle of the unit cell marked "B" in fig. 5 is displaced relative to the adjacent blocks that border iodine-containing layers. Consequently, the c-axis parameter of the stage-3 iodine-intercalated compound is longer than those of the host material and the stage-1 iodine-intercalated compound, but shorter than that of the stage-2 iodine-intercalated compound; these differences are summarized schematically in fig. 6.

Higher stage phases such as those appearing as stacking faults in fig. 1 seem to bear similar structural characteristics to the lower stage intercalates. For example, the stage-4 iodine-intercalated phase has four basic building blocks with a staggered stack-

ing sequence between two iodine layers across which the building blocks are in registry, to form the stacking sequence: A–I–A–B–A–B–I–B–A–B–A–I–A. The stage-5 iodine-intercalated phase would therefore be expected to have five basic building blocks with the staggered stacking sequence between 2 iodine layers across which the building blocks are in registry, to form the stacking sequence: A–I–A–B–A–B–A–I–A. Consequently, the stage-5 phase has a shorter c-axis dimension than the stage-4 phase since the registration of building blocks in the stage-5 phase does not require a doubling of the c-axis parameter to complete a unit cell. Since any single intercalated iodine layer expands the distance between Bi–O layers by 3.6 Å and since the length of a basic building block along the c-axis is 15.3 Å, it follows that the c parameter of the stage-4 phase should be 129.6 Å and that of the stage-5 phase should be 80.1 Å. These values correspond to the actual dimensions measurable in fig. 1. It ic concluded from these results that the c-axis dimension of a general stage-n iodine-intercalated phase is $m(3.6+15.3n)$ Å where $m=1$ when n is odd and $m=2$ when n is even (cf. fig. 6). Considering the stacking sequence of iodine layers and basic building blocks in the stage-1, stage-2 and stage-3 iodine-intercalated compounds, it is also possible to surmise the space group of a stage-n compound to be Pma2 when n is odd or Bbmb when n is even.

Figure 7 is another high-resolution transmission electron microscope image revealing even higher-stage iodine-intercalated phases than those discussed so far, i.e. stage numbers 4, 5, 6, 7, 10, 11, and 20 appear in the same field of view (see labels in fig. 7). The incident direction of the electron beam in this image is $[\bar{1}10]$. For each intercalate, the measured c-axis dimension agrees well with the above formula. Note also that the image also captures a two phase interface at the position marked "D" where a single intercalated iodine layer is responsible for the transformation of the stage-20 phase into two unit cells of stage-10 phase. There is considerable lattice distortion accompanying the 3.6 Å expansion of the crystal due to the localized intercalation of iodine, which induces both a compressive stress along the c-axis and a pure shear in the a–b plane, as seen in the image.

Table 2 summarizes the lattice parameters, space groups and the distances between adjacent cation layers in the pristine crystal and iodine-intercalated compounds. It is seen that although the presence of iodine expands the distance between the Bi–O layers between which it intercalates and causes a shift of the basic building blocks along the a- or b-axes by half of their lattice parameters, it causes no fundamental structural changes within the building blocks themselves. This behavior of the iodine is associated with its formation of weak van der Waals bonds to adjacent atomic layers.

Table 2
Comparison of the lattice parameters (Å), space groups and distances (Å) between adjacent cation layers in the host superconducting $Bi_2Sr_2CaCu_2O_x$ and the iodine-intercalated superconductors. The distances between the layers are defined using the z coordinates of the cations

	Pristine $Bi_2Sr_2CaCu_2O_x$	Stage-1 $IBi_2Sr_2CaCu_2O_x$	Stage-2 $IBi_4Sr_4Ca_2Cu_4O_x$	Stage-3 $IBi_6Sr_6Ca_3Cu_6O_x$	Stage-n $IBi_{2n}Sr_{2n}Ca_nCu_{2n}O_x$
a	5.4	5.4	5.4	5.4	5.4
b	5.4	5.4	5.4	5.4	5.4
c	30.6	18.9	68.5	49.4	$m(3.6+15.3n)$ $m=1$ when n is odd $m=2$ when n is even
Space group	Bbmb	Pma2	Bbmb	Pma2	Pma2 when n is odd Bbmb when n is even
I–Bi	–	3.31	3.40	3.40	3.40
Bi–(I)–Bi	3.24	6.62	6.80	6.80	6.80
Bi–Sr	2.70	2.80	2.70	2.70	2.70
Sr–Cu	1.70	1.70	1.70	1.70	1.70
Cu–Ca	1.65	1.65	1.65	1.65	1.65

Acknowledgements

The Atomic Resolution Microscope, image analysis facilities, and technical support at the National Center for Electron Microscopy are gratefully acknowledged. This research is supported by the Director, Office of Energy Research. Office of Basic Energy Sciences, Materials Sciences Division, of the US Department of Energy under Contract No. DE-AC03-76SF00098. JLC and MLC are supported by Natural Science Foundation Grant No. DMR88-18404. JLC acknowledges support from AT&T Bell Laboratories.

References

[1] X.-D. Xiang, S. McKernan, W.A. Vareka, A. Zettl, J.L. Corkill, T.W. Barbee III and M.L. Cohen, Nature 348 (1990) 145.

[2] X.-D. Xiang, A. Zettl, W.A. Vareka, J.L. Corkill, T.W. Barbee III and Marvin L. Cohen, Phys. Rev. B 43 (1991) 11496.

[3] X.-D. Xiang, W.A. Vareka, A. Zettl, J.L. Corkill, T.W. Barbee III, Marvin L. Cohen, N. Kijima and R. Gronsky, Science, submitted.

[4] N. Kijima, R. Gronsky, X.-D. Xiang, W.A. Vareka, A. Zettl, J.L. Corkill and Marvin L. Cohen, Physica C, submitted.

[5] N. Kijima, R. Gronsky, X.-D. Xiang, W.A. Vareka, A. Zettl, J.L. Corkill and M.L. Cohen, Physica C, submitted.

[6] W.O. Saxton, T.J. Pitt and M. Horner, Ultramicroscopy 4 (1979) 343.

[7] R. Kilaas, in: Proc. 45th Annual Meeting of the Electron Microscopy Society of America, ed. G.W. Bailey, Baltimore, Md. (1987) 66.